# Combined Iterative Demodulation and Decoding using very short LDPC Codes and Rate-1 Convolutional Codes

Thorsten Clevorn, Frank Oldewurtel[1], and Peter Vary
Institute of Communication Systems and Data Processing (ind)
RWTH Aachen University, Germany
{clevorn,vary}@ind.rwth-aachen.de

*Abstract* — **We propose the serial concatenation of a set of very short LDPC code blocks with components of rate 1. As second component we use a higher order modulation with a sophisticated mapping, a rate-1 convolutional code, or a serial concatenation of both. With this rate-1 component extrinsic information is exchanged between the LDPC code blocks resulting in a very good bit-error rate performance. The LDPC code blocks and each serial concatenation is separately but simultaneously iteratively decoded. Despite its relative low complexity, simulations show a competitive performance of the proposed system, e.g., compared to the UMTS Turbo code or a single, fixed LDPC code. Since the number of LDPC code blocks is flexible, the overall frame size can be adjusted with a high granularity.**

## I. Introduction

With the discovery of Turbo codes [1],[2],[3] and the (re-)discovery of low-density parity check (LDPC) codes [4],[5] channel coding close to the Shannon limit becomes possible with moderate computational complexity. One drawback of LDPC codes is the limited flexibility in terms of frame size. For each frame size a specific generator matrix and a corresponding parity-check matrix have to be generated. However, in modern communication systems the frame size is frequently adapted to the current user requirements and surrounding scenario.

In this contribution we present systems which use LDPC codes and allow to adjust the frame size with a high granularity. Instead of one long LDPC code a very short LDPC code is applied subsequently to a large and adjustable number of small sub-frames. To enable an information exchange between the sub-frames, the sub-frames are serially concatenated via an interleaver with a second component providing extrinsic information according to the Turbo principle. Properties of single short LDPC codes are discussed, e.g., in [6],[7].

For the system denoted as system "A" and presented in Section II a demodulator serves as second component. This resembles *bit-interleaved coded modulation with iterative decoding* (BICM-ID, or BICMID to simplify the notation in the following) [8], except that the used channel code, i.e., the LDPC code, is additionally iteratively decoded by itself. The simulation results for this LDPC-BICMID system given in Section III visualize that the gains of *iterative decoding* of the LDPC code and *iterative demodulation* can be combined.

In the system "B" introduced in Section IV the (de-)modulator is replaced by a convolutional code with its respective decoder. Thus, this system is independent of the used modulation. To avoid an increase in data rate by the new inner code and the inherent capacity loss by rate $< 1$ codes in serial concatenation [9], we use a rate-1 recursive non-systematic convolutional (RNSC) code. The simulation results for this LDPC-RNSC system depicted in Section V show significant gains, especially for low-memory, i.e., low-complex, RNSC codes. Furthermore, a comparison with an UMTS simulation reveals a competitive performance of the proposed LDPC-RNSC system.

In Section VI we finally combine the two previously described systems A and B to a third system "A+B", which features three separate iterative loops. We denote this system A+B by LDPC-RNSC-BICMID and present simulation results.

## II. System A: The LDPC-BICMID System

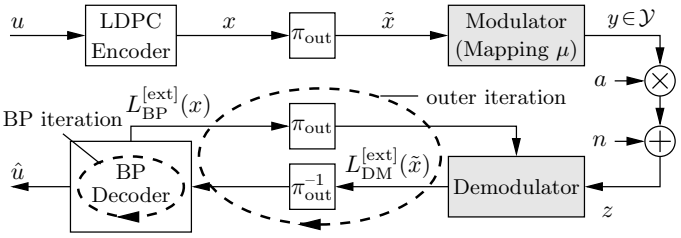


Figure 1: Baseband model of system A (LDPC-BICMID).

Fig. 1 depicts the baseband model of the system A (LDPC-BICMID) considered in this section of the paper. A block of data bits $u$ shall be encoded by an LDPC code. To ensure a high flexibility in the used block length, we do not use a single, large generator matrix. The frame of data bits $u$ is splitted in numerous small blocks, each encoded by a very short LDPC ("sub-")code. Being $\mathbf{G}_{\text{sub}}$ the generator matrix of the short LDPC code, the overall generator matrix $\mathbf{G}_{\text{LDPC}}$ is

$$\mathbf{G}_{\text{LDPC}} = \begin{pmatrix} \mathbf{G}_{\text{sub}} & 0 & 0 & \dots \\ 0 & \mathbf{G}_{\text{sub}} & 0 & \dots \\ 0 & 0 & \ddots & 0 \\ \vdots & \vdots & 0 & \mathbf{G}_{\text{sub}} \end{pmatrix} \tag{1}$$

For simplicity we assume that all $\mathbf{G}_{\text{sub}}$ are identical. However, otherwise for each LDPC code only a different decoder would be required. If, e.g., $U_L$ blocks encoded by an $(N,M)$-LDPC code are combined, in total a frame of $U = U_L \cdot M$ data bits $u$ is encoded to $X = U_L \cdot N$ encoded bits $x$, which are permuted to $\tilde{x}$ by a single pseudo-random bit-interleaver $\pi_{\text{out}}$ of size $U_L \cdot N$. Thus, the overall frame size of the data bits can be flexibly adjusted by a step size of $M$. The permuted bits are grouped consecutively into bit patterns $\underline{\tilde{x}}_t = [\tilde{x}_t^{(1)}, \dots \tilde{x}_t^{(I)}]$, where $\tilde{x}_t^{(i)}$

[1]Frank Oldewurtel is now with the Institute for Wireless Networks, RWTH Aachen University; fol@mobnets.rwth-aachen.de

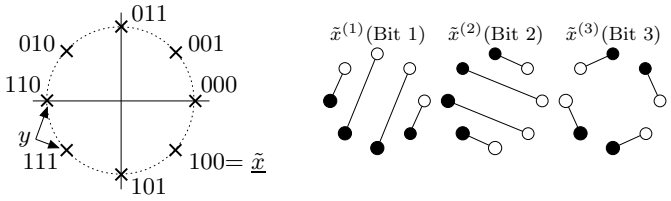


Figure 2: 8PSK-Gray with EFF decision distances.

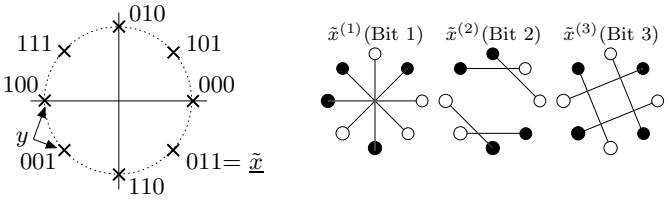


Figure 3: 8PSK-SSP with EFF decision distances.

denotes the $i^{\text{th}}$ bit in the bit pattern at time index $t$, $t=1,...T$. $I$ is the number of bits that will be mapped to one channel symbol later on, e.g., $I=3$ in case of 8PSK. In case the last bit pattern is not completely filled, i.e., $U_L \cdot N \mod I \neq 0$, the remaining positions are padded by zeros.

The modulator maps an interleaved bit pattern $\underline{\tilde{x}}_t$ according to a mapping rule $\mu$ to a complex channel symbol $y_t$ out of the signal constellation set (SCS) $\mathcal{Y}$

$$y_t = \mu(\underline{\tilde{x}}_t) \quad . \tag{2}$$

The respective inverse relation is denoted by $\mu^{-1}$, with

$$\underline{\tilde{x}}_t = \mu^{-1}(y_t) = [\mu^{-1}(y_t)^{(1)}, ... \mu^{-1}(y_t)^{(I)}] \quad . \tag{3}$$

The channel symbols are normalized to an average energy of $E_s = E\{\|y_t\|^2\} = 1$. The transmitted symbols $\tilde{y}_t$ are faded by the Rayleigh distributed coefficients $a_t$ with $E\{\|a_t\|^2\} = 1$. In this contribution we assume that these coefficients are known at the receiver, i.e., perfect knowledge of the channel state information (CSI). Next, complex zero-mean white Gaussian noise $n_t = n_t' + jn_t''$ with a known power spectral density of $\sigma_n^2 = N_0$ ($\sigma_{n'}^2 = \sigma_{n''}^2 = N_0/2$) is added. Thus, the received channel symbols $\tilde{z}_t$ can be written as

$$\tilde{z}_t = a_t \tilde{y}_t + n_t \quad . \tag{4}$$

The demodulator (DM) computes *extrinsic* probabilities $P_{\text{DM}}^{[\text{ext}]}(\tilde{x})$ for each bit $\tilde{x}_t^{(i)}$ being $b \in \{0,1\}$ according to [8]

$$P_{\text{DM}}^{[\text{ext}]}(\tilde{x}_t^{(i)}=b) \sim \sum_{\hat{y} \in \mathcal{Y}_b^i} P(z_t|\hat{y}) P_{\text{BP}}^{[\text{ext,i}]}(\hat{y}) \quad , \tag{5}$$

$$\text{with} \quad P_{\text{BP}}^{[\text{ext,i}]}(\hat{y}) \triangleq \prod_{j=1, j\neq i}^{I} P_{\text{BP}}^{[\text{ext}]}\left(\tilde{x}_t^{(j)} = \mu^{-1}(\hat{y})^{(j)}\right) \quad . \tag{6}$$

Each $P_{\text{DM}}^{[\text{ext}]}(\tilde{x})$ consists of the sum over all possible channel symbols $\hat{y}$ for which the $i^{\text{th}}$ bit of the corresponding bit pattern $\underline{\tilde{x}} = \mu^{-1}(\hat{y})$ is $b$. These channel symbols form the subset $\mathcal{Y}_b^i$ with $\mathcal{Y}_b^i = \{\mu([\tilde{x}^{(1)}, ... \tilde{x}^{(I)}]) | \tilde{x}^{(i)} = b\}$. The two $P_{\text{DM}}^{[\text{ext}]}(\tilde{x})$ for $\tilde{x} = \{0,1\}$ are combined to one L-value [2] $L_{\text{DM}}^{[\text{ext}]}(\tilde{x})$.

In the first iteration the feedback probabilities $P_{\text{BP}}^{[\text{ext}]}(\tilde{x})$ obtained from the feedback L-value $L_{\text{BP}}^{[\text{ext}]}(\tilde{x})$ are initialized as equiprobable, i.e., $P_{\text{BP}}^{[\text{ext}]}(\tilde{x}) = 0.5$. The conditional probability density $P(z_t|\hat{y})$ describing the Rayleigh channel is given by

$$P(z_t|\hat{y}) = \frac{1}{\pi\sigma_n^2} \exp(-\|z_t - a_t\hat{y}\|^2/\sigma_n^2) \quad . \tag{7}$$

After appropriately deinterleaving the $L_{\text{DM}}^{[\text{ext}]}(\tilde{x})$ to $L_{\text{DM}}^{[\text{ext}]}(x)$, the $L_{\text{DM}}^{[\text{ext}]}(x)$ are fed into the $U_L$ separate belief propagation (BP) decoders for the small LDPC encoded blocks. Each BP decoder performs a certain number of "BP iterations" $\Xi_{\text{BP}}$ and computes *extrinsic* information $L_{\text{BP}}^{[\text{ext}]}(x_t^{(i)})$ for the encoded bits in addition to the preliminary estimated decoded data bits $\hat{u}$. For details on possible implementations for the BP decoder using L-values, i.e., the sum-product algorithm (SPA) and its approximations, we refer to the literature, e.g., [10],[11],[12],[13].

For the next iteration between BP decoder and demodulator the $L_{\text{BP}}^{[\text{ext}]}(x)$ are interleaved again to $L_{\text{BP}}^{[\text{ext}]}(\tilde{x})$ in order to be fed into the demodulator. We denote this iteration as "outer iteration" $\Xi_{\text{out}}$. Thus, in one outer iteration $\Xi_{\text{out}}$ each BP decoder executes one or more BP iterations $\Xi_{\text{BP}}$.

If the channel is sufficiently good and enough outer iterations are performed, the feedback values $L_{\text{BP}}^{[\text{ext}]}(\tilde{x})$ are such reliable that they can be considered as error-free feedback (EFF) [8]. With this EFF, the demodulation degenerates to a simple BPSK decision for each bit. For example, assuming the 8PSK-Gray mapping depicted in Fig. 2 and the EFF is $\tilde{x}^{(2)} = 1$ and $\tilde{x}^{(3)} = 1$, the demodulator makes a soft decision for bit $\tilde{x}^{(1)}$ only between $\underline{\tilde{x}} = 111$ and $\underline{\tilde{x}} = 011$. These decision distances are depicted on the right side of Fig. 2, where a black dot denotes $\tilde{x}^{(i)} = 1$ and a white dot $\tilde{x}^{(i)} = 0$. Obviously, the larger the distances are, the more reliable the decision will be. Gray mapping, which is optimum mapping for the non-iterative BICM case [14], usually allows none or only a small gain by iterative demodulation. For the iterative BICMID other mappings have to be used. The optimum mapping for a regular 8PSK signal constellation set (SCS) is the Semi-Set Partitioning (SSP) mapping [8] depicted in Fig. 3. Further mappings are presented, e.g., in [15],[16].

For a detailed analysis of BICMID we refer again to the literature, e.g., [8],[15],[16]. Nevertheless, in case of a Rayleigh channel and the same channel code all mappings exhibit a linear slope of the error floor with a constant horizontal offset in between. This offset solely depends on the harmonic mean of the squared EFF decision distances, which are depicted, e.g., on the right sides of Figs. 2 and 3. The horizontal offset measured in dB with respect to the optimum non-iterative BICM case is called *offset gain* $\mathcal{G}$ [8]. As mentioned in the previous paragraph, the *offset gain* of Gray mappings is almost negligible, e.g., $\mathcal{G}(\text{8PSK-Gray}) = 0.24$ dB. In contrast, e.g., the 8PSK-SSP mapping offers a significant *offset gain* of $\mathcal{G}(\text{8PSK-SSP}) = 5.74$ dB. Thus, the error floor of BICMID with 8PSK-SSP mapping will be about 5.5 dB superior to the one with 8PSK-Gray mapping.

## III. Results for System A (LDPC-BICMID)

The results of a bit-error rate (BER) simulation for system A (LDPC-BICMID) with a Rayleigh channel are depicted in Fig. 4. 8PSK is used as SCS with Gray or SSP [8] mapping. Novel SCSs and mappings, and the advantages of PSK SCSs are discussed in [17],[18]. As LDPC code serves a difference-set cyclic (DSC) code, the (21,11)-DSC code. DSC codes are a special class of LDPC codes which exhibits good performance for short block length [10]. A frame of $U = 990$ data bits is split into $U_L = 90$ small blocks and

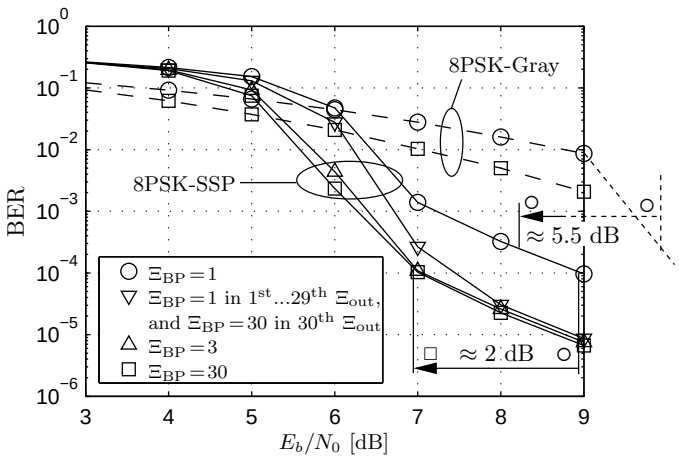


Figure 4: BER for system A (LDPC-BICMID), Rayleigh channel, (21,11)-DSC code, frame size $U=990$ and $X=1890$, $\Xi_{out}=30$ outer iterations.

then encoded to in total $X = 1890$ bits. The total code rate is $r_{DSC}=M/N=U/X\approx 0.524$. In the BP decoder the non-approximated SPA is used. Each time $\Xi_{out}=30$ outer iterations are executed with a varying number $\Xi_{BP}$ of BP iterations for the different curves.

For the curves labeled "○" only one BP iteration is performed in each outer iteration. This resembles a classic BICMID system with a channel code, which is not iterative by itself. The typical offset gain between the error floors of the different mapping can be observed. This is the gain obtainable by *iterative demodulation*. The not displayed results for $E_b/N_0>9$ dB show that in the error floor region the SSP mapping outperforms Gray mapping approximately by the theoretically predicted offset gain difference of 5.5 dB. Note, this is the same gain, e.g., a standard convolutional code would achieve when switching from Gray to SSP mapping and applying *iterative demodulation*.

If in each outer iteration $\Xi_{BP}=30$ BP iterations are performed we obtain the results marked "□". As visible, an additional gain of $\Delta_{E_b/N_0}\approx 2$ dB can be achieved with respect to the BICMID case ("○"). Thus, this gain is realizable by internal *iterative decoding* for the LDPC channel code.

The curves "▽" and "△" show that this additional gain can be achieved also by fewer BP iterations, at least for BERs below $5\cdot 10^{-5}$. For "▽" in the first 29 outer iterations just a single BP iteration is executed, and only at the end of the last outer iteration the BP decoder iterates 30 times. Thus, with this setting the two different gains are separately realized, first, by the initial 29 outer iteration the gain by *iterative demodulation*, and afterwards in the final outer iteration the gain by *iterative decoding* due to the $\Xi_{BP}=30$ BP iterations. However, since in the first outer iterations the *iterative decoding* gain is not used the waterfall region starts at noticeably higher $E_b/N_0$ compared to "□". When using $\Xi_{BP}=3$ BP iterations in every outer iteration ("△") an *iterative decoding* gain can be obtained in every iteration and the results are only slightly inferior to "□", but with a ten times lower complexity.

## IV. System B: The LDPC-RNSC System

In Section II we presented the system A in which numerous small code blocks are connected by a large interleaver and iterative demodulation of higher order modulation. The demodulator acts as rate-1 code to exchange extrinsic information between the small blocks in a Turbo process. In case of no access to the demodulator for iterative demodulation or BPSK modulation, we propose the system B (LDPC-RNSC) depicted in Fig. 5, in which a rate-1 recursive non-systematic convolutional (RNSC) code is placed between LDPC encoder and Modulator. Still, the inner code has a code rate of 1 (or $\approx 1$ considering tail bits), which avoids a capacity loss inherent for serial concatenation with an inner code of a rate $<1$ [9]. The RNSC code is now responsible for information exchange between short LDPC code blocks. A similar concept is used in [19] for *Turbo error concealment*. Here the RNSC code is denoted as "smearing filter".

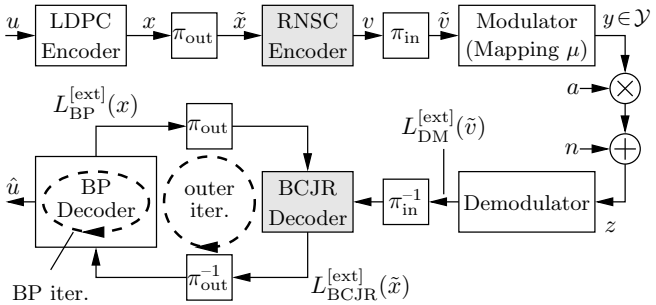


Figure 5: Baseband model of system B (LDPC-RNSC).

The rate-1 RNSC encoder has a memory of $J$, i.e., a constraint length of $J+1$. It encodes the LDPC encoded and permuted bits $\tilde{x}$ to $v$, which are permuted by a new *inner* bit-interleaver $\pi_{in}$. For BPSK modulation, i.e., $y=\pm 1$, the inner interleaver can be omitted. The RNSC uses termination by $J$ tail bits, leading to a rate of $r_{RNSC}=X/(X+J)\approx 1$. Thus, in total $V=X+J$ bits $v$ are transmitted via the same channel as in Section II. At the receiver a BCJR decoder [20] takes in the outer iterations the role of refining the extrinsic information $L_{BP}^{[ext]}$ from the BP decoders to $L_{BCJR}^{[ext]}$. The demodulator is not part of the iterative loop anymore and no gain by iterative demodulation is possible. Thus, in the following we use BPSK modulation for simplicity.

## V. Results for System B (LDPC-RNSC)

Figs. 6 and 7 depict results of BER simulations for system B (LDPC-RNSC) with BPSK modulation. Similar to Section III a frame of $U=990$ data bits is encoded using $U_L=90$ (21,11)-DSC encoders to a frame of $X=1890$ bits. The by $\pi_{out}$ permuted bits $\tilde{x}$ are encoded (including tail-bits) by a memory $J$ RNSC encoder with generator polynomial $\mathbf{G}_{RNSC}^{J}$. As generator polynomials we use $\mathbf{G}_{RNSC}^{1}=(\frac{1}{1+D})$, $\mathbf{G}_{RNSC}^{2}=(\frac{1}{1+D+D^2})$ and $\mathbf{G}_{RNSC}^{3}=(\frac{1}{1+D+D^2+D^3})$. At the receiver for each LDPC-RNSC frame $\Xi_{out}=20$ outer iterations are performed, with $\Xi_{BP}=3$ or $\Xi_{BP}=1$ BP iterations using the non-approximated SPA executed in each outer iteration.

As reference and for comparison three more results are depicted in both Figures. For the curve "○" the RNSC code is removed from the system and only $\Xi_{BP}=30$ iterations are executed by the BP decoder. Without the serial concatenation the small LDPC code blocks of length $N=21$ cannot exchange extrinsic information through outer iterations. This system is identical to one with a single (21,11)-DSC code applied to frames of size $U=M=11$. The curve "□" denotes a similar system, but with a single, fixed ($N=1890$,$M=990$)-LDPC

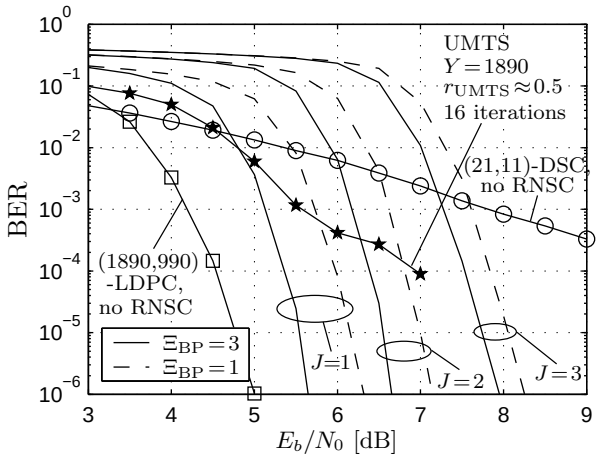


Figure 6: BER for system B (LDPC-RNSC), Rayleigh channel, BPSK, (21,11)-DSC code, frame size $U=990$, $X=1890$ and $V=1890+J$, $\Xi_{\mathrm{out}}=20$ outer iter. with $\Xi_{\mathrm{BP}}=3$ or $\Xi_{\mathrm{BP}}=1$ BP iterations each.

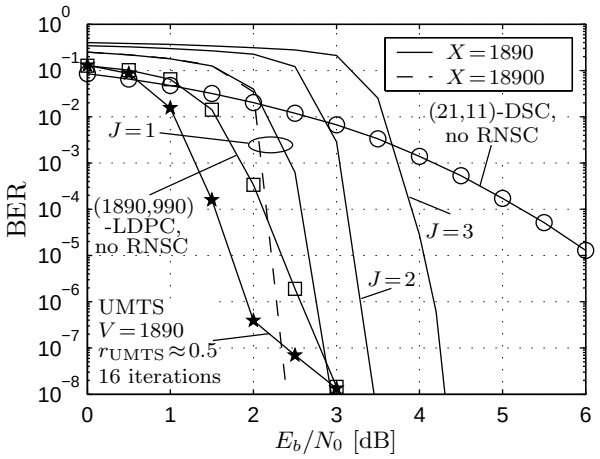


Figure 7: BER for system B (LDPC-RNSC), AWGN channel, BPSK, (21,11)-DSC code, frame size $U=990$, $X=1890$ and $V=1890+J$, $\Xi_{\mathrm{out}}=20$ outer iterations with $\Xi_{\mathrm{BP}}=3$ BP iterations each.

code, i.e., $U_L=1$. This code was generated using software provided at [21] and choosing a column weight of 3. The third curve ("$\star$") represents a system using the UMTS Turbo code. For the UMTS simulations we use CoCentric System Studio with the Design Conformance Lab for UMTS (FDD) by Synopsys, Inc. [22]. The original rate-1/3 Turbo code is punctured to an approximately similar rate $r_{\mathrm{UMTS}}=1/2$. The frame size is set to $V=1890$ bits and 16 iterations are carried out at the decoder using the Log-BCJR (or Log-MAP) algorithm. The component codes of the UMTS Turbo code are of memory 3 and thus require a trellis with 8 states.

In Fig. 6 the Rayleigh channel model is used for the simulations. As visible, system B (LDPC-RNSC) exhibits a steep waterfall region and no error floor, at least in the depicted BER region. For smaller $J$, i.e., an RNSC code with less memory and lower complexity, the results improve, with the waterfall region starting at a lower $E_b/N_0$. Due to the steepness in the waterfall region the systems with a larger memory $J$ cannot make up for this penalty in the useful BER range. Thus, the least complex system with $J=1$ performs best. Using $\Xi_{\mathrm{BP}}=3$ (solid curves) instead of $\Xi_{\mathrm{BP}}=1$ (dashed curves) BP iterations yields in a noticeable enhancement. With $\Xi_{\mathrm{BP}}=3$ the gain by iterative decoding of the LDPC code, i.e., improved extrinsic information, is used in every outer iteration. However, the gap closes for increasing RNSC code memory $J$. With a large $J$ the BCJR decoder can provide better extrinsic information if the system is operating in the waterfall region. Thus, the influence of the number of BP iterations $\Xi_{\mathrm{BP}}$ decreases.

In contrast to system B (LDPC-RNSC) the UMTS Turbo code reference system exhibits an obvious error floor. The best depicted system B with $J=1$ and $\Xi_{\mathrm{BP}}=3$ significantly outperforms the UMTS Turbo code below a BER of $10^{-2}$. To achieve an approximatively similar flexibility in terms of frame size, system B uses the very short LDPC ("sub-")codes. Thus, as explained above the frame size can be adjusted by a step size of $N$. Note that the complexity of system B is quite low. For the BP decoder numerous low-complexity algorithms exist, see e.g. [11],[12],[13]. Furthermore, the BP decoder operates only on the very short LDPC code blocks. With $J=1$ the trellis of the BCJR decoder consists of only 2 states. In comparison, the UMTS Turbo code requires two trellises with 8 states each. Thus, the BCJR decoder in the outer iteration does not increase the complexity of system B significantly with respect to a system using only one LDPC code and no RNSC code. Similar considerations can be made for the additional complexity by the iterative demodulation used in Sections II, III and VI. The iterative demodulation, i.e., equations (5) and (6) (equation (7) needs to be computed only once in all systems), for an 8PSK SCS has approximately the same computational complexity as a BCJR decoder for a 2-state trellis.

Fig. 7 presents the results for a simple AWGN channel, i.e., $a_t=1$. In analogy to the Rayleigh channel system in Fig. 6 an increase in memory $J$ for the RNSC code yields an inferior performance. The waterfall region for $J=1$ occurs at a $\approx 2.5$ dB lower $E_b/N_0$ compared to the Rayleigh case. Also the UMTS Turbo code reference system exhibits again an error floor. But it occurs at lower BERs than in the Rayleigh case and the UMTS system shows superior results compared to system B in a wide range of BERs. Nevertheless, the complexity considerations made for Fig. 6 still hold and at very low BERs system B performs best. For the dashed curve the frame size of system B with $J=1$ is increased by a factor of 10. As visible, for larger frames the results are further improved. The degradation of system B (LDPC-RNSC) compared to a single LDPC code of similar but non-flexible size (curve "$\square$") is smaller than 0.5 dB at BERs below $10^{-4}$. At very low BERs ($<10^{-7}$) system B is actually superior.

## VI. System A+B: The LDPC-RNSC-BICMID Syst.

Obviously, if the modulator uses a large SCS $\mathcal{Y}$ such as 8PSK, the system B (LDPC-RNSC) presented in Section IV and the system A (LDPC-BICMID) introduced in Section II can be merged into a system A+B (LDPC-RNSC-BICMID). The baseband model of the emerging system A+B is depicted in Fig. 8. This time two interleavers are required. An *outer* interleaver $\pi_{\mathrm{out}}$ for the LDPC encoded bits $x$ and an *inner* interleaver $\pi_{\mathrm{in}}$ for the RNSC encoded bits $v$. At the receiver there exist now two iterative loops in addition to the internal BP iterations. In the *outer* iteration $\Xi_{\mathrm{out}}$ between BP decoder and BCJR decoder *extrinsic* information on the bits $x$

is exchanged, while the *inner* iterations $\Xi_{\text{in}}$ between demodulator and BCJR decoder pass *extrinsic* information on the bits $v$. Note that the BCJR decoder has to be modified to generate the two different *extrinsic* informations $L^{[\text{ext}]}_{\text{BCJR}}(\tilde{x})$ and $L^{[\text{ext}]}_{\text{BCJR}}(v)$. For the order of inner and outer iterations there exist several possibilities. For simplicity we restrict ourselves to the case in which both are executed in parallel, i.e., the BCJR decoder feeds both iterative loops simultaneously.

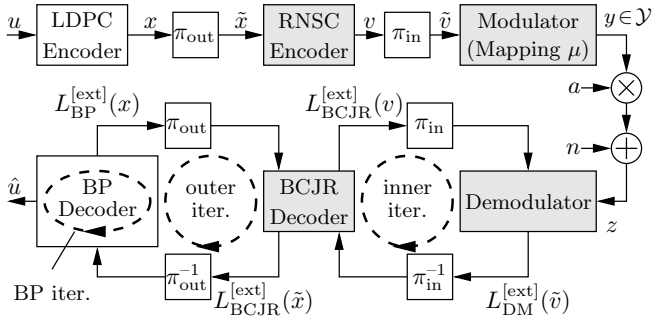


Figure 8: Baseband model of system A+B (LDPC-RNSC-BICMID).

In Fig. 9 BER simulation results of system A+B (LDPC-RNSC-BICMID) are depicted. The parameter settings are similar to the previous simulations in Sections III and V. $\Xi_{\text{out}} = \Xi_{\text{in}} = 20$ outer and inner iterations are performed with $\Xi_{\text{BP}} = 3$ BP iterations per outer iteration. For the memory of the RNSC we use the optimum case of $J = 1$. In contrast to system A (LDPC-BICMID), 8PSK-Gray mapping significantly outperforms 8PSK-SSP in this case. This is a result of the very steep waterfall region generated by the outer iterations. The error floor, at which 8PSK-SSP would be superior, is at such low BERs that it is not reached for realistic BERs. Furthermore, since the 8PSK-Gray mapping does not profit a lot from iterative demodulation, the performance loss by omitting the inner iterations, i.e., $\Xi_{\text{in}} = 1$, is negligible as visible for the AWGN case with 8PSK-Gray in Fig. 9.

## VII. Conclusion

In this paper we proposed several systems consisting of a serial concatenation of lots of very short LDPC code blocks with components of rate 1. This second component can either be a higher order modulation with a sophisticated mapping, a rate-1 convolutional code, or a serial concatenation of both. At the receiver each serial concatenation is iteratively decoded, with an additional iterative loop in the belief propagation decoder for the LDPC code. The rate-1 components enable an information exchange between the short LDPC code blocks, leading to a competitive BER performance of all systems. Comparisons for the system using a rate-1 convolutional code with the UMTS Turbo code reveal the following advantages:

- superior BER performance for a Rayleigh channel,
- no error floor at realistic BERs,
- low complexity (2-state trellis and BP decoder),
- highly flexible overall frame size,
- small degradation compared to a single, fixed LDPC code (actually superior performance at very low BERs).

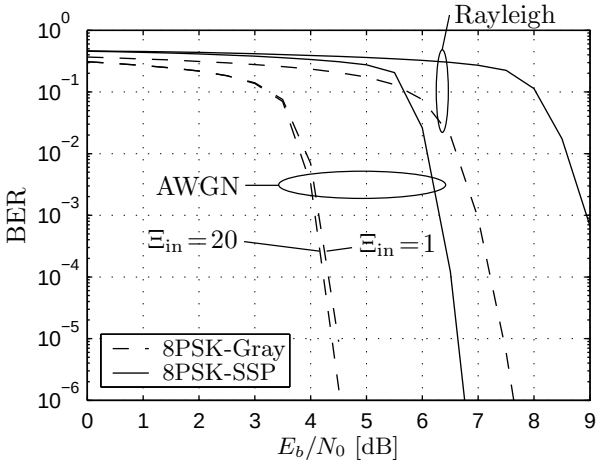


Figure 9: BER for system A+B (LDPC-RNSC-BICMID), (21,11)-DSC code, $J = 1$, 8PSK, frame size $U = 990$, $X = 1890$ and $V = 1891$, Rayleigh or AWGN channel, $\Xi_{\text{out}} = 20$ outer iterations with $\Xi_{\text{BP}} = 3$ BP iterations each, $\Xi_{\text{in}} = 20$ inner iterations.

## References


[1] C. Berrou and A. Glavieux, "Near Optimum Error Correcting Coding and Decoding: Turbo-Codes," *IEEE Trans. Comm.*, Oct. 1996.

[2] J. Hagenauer, E. Offer, and L. Papke, "Iterative Decoding of Binary Convolutional Codes," *IEEE Trans. Inform. Theory*, pp. 429–445, Mar. 1996.

[3] S. Benedetto, D. Divsalar, G. Montorsi, and F. Pollara, "Serial Concatenation of Interleaved Codes: Performance Analysis, Design, and Iterative Decoding," *IEEE Trans. Inform. Theory*, pp. 909–921, May 1998.

[4] D. J. C. MacKay, "Good Error-Correcting Codes Based on Very Sparse Matrices," *IEEE Trans. Inform. Theory*, pp. 399–431, Mar. 1999.

[5] R. G. Gallager, "Low-Density Parity-Check Codes," *IRE Trans. Inform. Theory*, pp. 21–28, Jan. 1962.

[6] L. Wei, "Several Properties of Short LDPC Codes," *IEEE Trans. Comm.*, pp. 721–727, May 2004.

[7] W. Wu, S. Hong, and D.-S. Yoo, "Block Length of LDPC Codes in Fading Channels," *IEEE 57th Vehicular Technology Conference (VTC Spring)*, Jeju, Korea, Apr. 2003.

[8] X. Li, A. Chindapol, and J. A. Ritcey, "Bit-Interleaved Coded Modulation With Iterative Decoding and 8PSK Signaling," *IEEE Trans. Comm.*, pp. 1250–1257, Aug. 2002.

[9] A. Ashikhmin, G. Kramer, and S. ten Brink, "Extrinsic information transfer functions: model and erasure channel properties," *IEEE Trans. Inform. Theory*, pp. 2657–2673, Nov. 2004.

[10] R. Lucas, M. P. Fossorier, Y. Kou, and S. Lin, "Iterative Decoding of One-Step Majority Logic Decodable Codes Based on Belief Propagation," *IEEE Trans. Comm.*, pp. 931–937, June 2000.

[11] X.-Y. Hu, E. Eleftheriou, D.-M. Arnold, and A. Dholakia, "Efficient Implementations of the Sum-Product Algorithm for Decoding LDPC Codes," *Globecom 2001*, San Antonio, TX, USA, Nov. 2001.

[12] T. Clevorn and P. Vary, "Low-Complexity Belief Propagation by Approximations with Lookup-Tables," *5th Intern. ITG Conf. on Source and Channel Coding (SCC)*, Erlangen, Germany, Jan. 2004.

[13] T. Clevorn and P. Vary, "The Box-Minus Operator and its Application to Low-Complexity Belief Propagation Decoding," *IEEE 61st Vehicular Technology Conference (VTC Spring)*, Stockholm, Schweden, May 2005.

[14] G. Caire, G. Taricco, and E. Biglieri, "Bit-Interleaved Coded Modulation," *IEEE Trans. Inform. Theory*, pp. 927–946, May 1998.

[15] T. Clevorn and P. Vary, "Iterative Decoding of BICM with Non-Regular Signal Constellation Sets," *5th Intern. ITG Conf. on Source and Channel Coding (SCC)*, Erlangen, Germany, Jan. 2004.

[16] F. Schreckenbach, N. Görtz, J. Hagenauer, and G. Bauch, "Optimized Symbol Mappings for Bit-Interleaved Coded Modulation with Iterative Decoding," *Globecom 2003*, San Francisco, Dec. 2003.

[17] T. Clevorn, S. Godtmann, and P. Vary, "PSK versus QAM for Iterative Decoding of Bit-Interleaved Coded Modulation," *Globecom 2004*, Dallas, Dec. 2004.

[18] T. Clevorn, S. Godtmann, and P. Vary, "EXIT Chart Analysis of Non-Regular Signal Constellation Sets for BICM-ID," *International Symposium on Information Theory and its Applications (ISITA 2004)*, Parma, Italy, Oct. 2004.

[19] M. Adrat and P. Vary, "Iterative Source-Channel Decoding with Code Rates Near $r=1$," *IEEE International Conference on Communications (ICC 2004)*, Paris, France, June 2004.

[20] L. R. Bahl, J. Cocke, F. Jelinek, and J. Raviv, "Optimal Decoding of Linear Codes for Minimizing Symbol Error Rate," *IEEE Trans. Inform. Theory*, pp. 284–287, Mar. 1974.

[21] D. J. C. MacKay, "Encyclopedia of Sparse Graph Codes," available at *http://www.inference.phy.cam.ac.uk/mackay/codes/data.html*.

[22] *Design Conformance Lab for UMTS (FDD), Reference Manual*, Synopsys, Inc., Dec. 2002.